

Matrix Isolation Infrared Spectroscopic and Density Functional Theory Studies on the Reactions of Dysprosium Hydride with Carbon Monoxide

Yun-Lei Teng and Qiang Xu*

National Institute of Advanced Industrial Science and Technology (AIST), Ikeda, Osaka 563-8577

Graduate School of Engineering, Kobe University, Nada-ku, Kobe, Hyogo 657-8501

Received March 24, 2008; E-mail: q.xu@aist.go.jp

Laser-ablated dysprosium hydride has been co-deposited at 4 K with carbon monoxide in excess argon. Product HDyCO has been formed in the present experiments and characterized using infrared spectroscopy on the basis of the results of the isotopic shifts, mixed isotopic splitting patterns, stepwise annealing, and the comparison with theoretical predictions. Density functional theory calculations have been performed. The agreement between the experimental and calculated vibrational frequencies, and isotopic shifts supports the identification of the molecule from the matrix infrared spectra. A plausible reaction mechanism has been proposed to account for the formation of this molecule.

The bonding of carbon monoxide with transition metals and transition-metal compounds is of great interest because of the importance of metal carbonyls in a great number of metal-catalyzed reactions.^{1–3} The long-standing goal of elucidating mechanisms of catalytic reactions involving CO has motivated numerous experimental and theoretical investigations of the interactions of metals with CO.⁴ The reactions of laser-ablated lanthanoid metals with carbon monoxide have been extensively studied.⁵

Metal hydrides are important as hydrogen storage materials for fuel cells.^{6a} For instance, a LaNi₅ alloy has been found to reversibly absorb/desorb hydrogen.^{6b,6c} The reactions of laser-ablated Dy with molecular hydrogen in excess argon have been reported and the products DyH₄ and DyH₂ have been characterized by infrared spectroscopy.⁷ On the other hand, a number of important metal-catalyzed reactions using syn-gas, such as methanol synthesis, the oxo process and Fischer–Tropsch synthesis, involve metal–carbonyl–hydride species as the reaction intermediates.^{8a} There have been reports of metal–carbonyl–hydride complexes such as HW(CO)₂,^{8b} H₂M(CO)₄ (M = Fe, Ru, and Os), and HCo(CO)₄.^{8c–8e} Such metal–carbonyl–hydride species may also play an important role in the degradation of anode catalyst of polymer electrolyte fuel cells (PEFCs) using hydrogen containing CO impurity produced from steam reforming or the partial oxidation of alcohols or hydrocarbons.⁹ As a rare example, the reactions of laser-ablated ruthenium atoms with carbon monoxide and hydrogen in solid argon have been recently investigated, and the products, such as the ruthenium carbonyl dihydride H₂Ru(CO)₂ and the hydrogen complexes (H₂)_xRuCO (*x* = 1 and 2), have been observed.¹⁰ In addition, we have reported the reactions of laser-ablated yttrium and lanthanum hydrides with carbon monoxide in a solid-argon matrix and the products, HYCO, (HY)₂CO, HLaCO, HLa(CO)₂, and H₂LaCO have been characterized.¹¹

Recent studies have shown that, with the aid of isotopic substitution techniques, matrix isolation infrared spectroscopy combined with quantum chemical calculation is very powerful for investigating structure and bonding of novel species.^{4,12} To understand the formation of carbonyl–hydride species of dysprosium, the reactions of laser-ablated dysprosium hydride with carbon monoxide in solid-argon matrix have been performed. IR spectroscopy and theoretical calculations provide evidence for the formation of product HDyCO.

Experimental and Theoretical Methods

The experiment for laser ablation and matrix-isolation infrared spectroscopy is similar to those previously reported.¹² Briefly, the Nd:YAG laser fundamental (1064 nm, 10 Hz repetition rate with 10 ns pulse width) was focused on the rotating DyH_x (>99%, High Purity Chemicals) target. The laser-ablated species were co-deposited with CO in excess argon onto a CsI window cooled normally to 4 K by means of a closed-cycle helium refrigerator (V24SC6LSCP, Daikin Industries). Typically, a 3–30 mJ pulse^{−1} laser power was used. Carbon monoxide (99.95% CO), ¹³C¹⁶O (99%, ¹⁸O <1%), and ¹²C¹⁸O (99%) were used to prepare the CO/Ar mixtures. In general, matrix samples were deposited for 30–60 min with a typical rate of 2–4 mmol per hour. After sample deposition, IR spectra were recorded on a BIO-RAD FTS-6000e spectrometer at 0.5 cm^{−1} resolution using a liquid nitrogen cooled HgCdTe (MCT) detector for the spectral range of 5000–400 cm^{−1}. Samples were annealed at different temperatures.

Quantum chemical calculations were performed to predict the structure and vibrational frequencies of the observed reaction product using the Gaussian 03 program.¹³ The BPW91 and BP86 density functional methods were utilized.¹⁴ The 6-311+G(d) basis set which involves polarized and diffuse functions was used for H, C, and O atoms.¹⁵ The SDD basis set with CEP effective core potential was used for Dy (28 core electrons).¹⁶ Geometries were fully optimized and vibrational frequencies were calculated with analytical second derivatives.

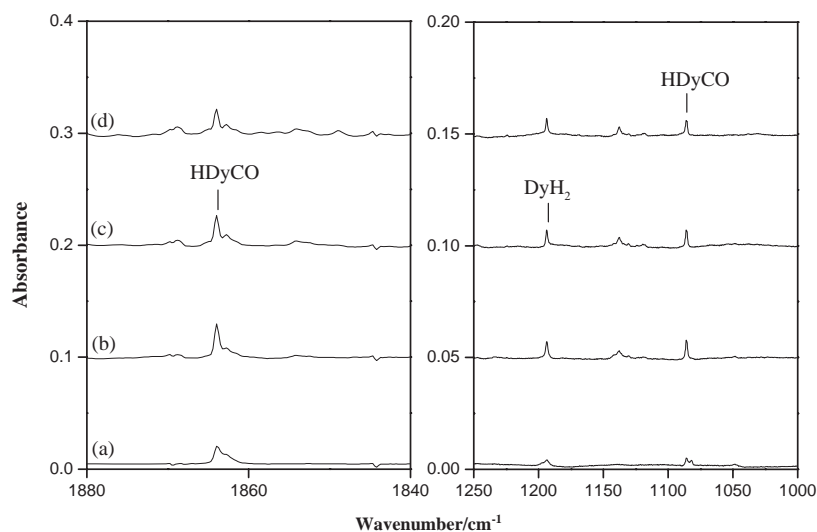


Figure 1. Infrared spectra in the 1880–1840 and 1250–1000 cm^{-1} regions from co-deposition of laser-ablated dysprosium hydride with 0.3% CO in argon: (a) 1 h sample deposition at 4 K; (b) after annealing to 25 K; (c) after annealing to 30 K; (d) after annealing to 35 K.

Table 1. Infrared Absorptions (cm^{-1}) from Co-Deposition of Laser-Ablated DyH_x with CO in Excess Argon at 4 K

$^{12}\text{C}^{16}\text{O}$	$^{13}\text{C}^{16}\text{O}$	$^{12}\text{C}^{18}\text{O}$	$^{12}\text{C}^{16}\text{O} + ^{13}\text{C}^{16}\text{O}$	$^{12}\text{C}^{16}\text{O} + ^{12}\text{C}^{18}\text{O}$	$R(12/13)$	$R(16/18)$	Assignment ^{a)}
1864.0	1823.9	1819.0	1863.9, 1823.9	1864.0, 1819.1	1.0220	1.0247	HDyCO, CO str.
1086.0	1079.8	1082.5	1086.0, 1079.9	1086.0, 1082.6			HDyCO, DyH str.

a) str. = stretching mode.

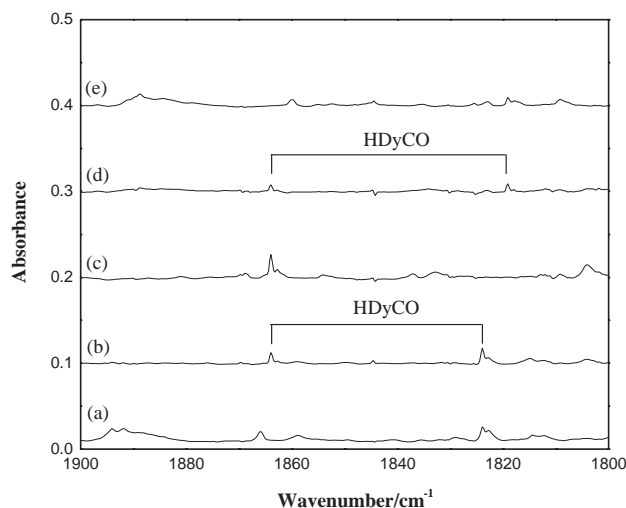


Figure 2. Infrared spectra in the 1900–1800 cm^{-1} region from co-deposition of laser-ablated dysprosium hydride with CO in argon after annealing at 30 K: (a) 0.3% $^{13}\text{C}^{16}\text{O}$; (b) 0.15% $^{12}\text{C}^{16}\text{O} + 0.15\%$ $^{13}\text{C}^{16}\text{O}$; (c) 0.3% $^{12}\text{C}^{16}\text{O}$; (d) 0.15% $^{12}\text{C}^{16}\text{O} + 0.15\%$ $^{12}\text{C}^{18}\text{O}$; (e) 0.3% $^{12}\text{C}^{18}\text{O}$.

Results and Discussion

Experiments were performed with CO concentrations ranging from 0.05% to 0.5% in excess argon. Typical infrared spectra for the reactions of laser-ablated DyH_x with CO in excess argon in the selected regions are illustrated in Figures 1 and 2, and the absorption bands are listed in Table 1. The

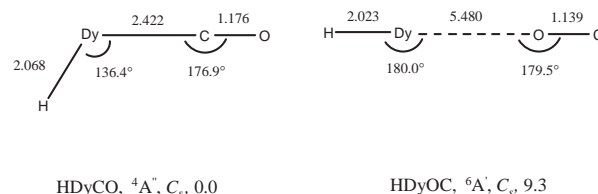


Figure 3. Optimized structures (bond length in Å, bond angle in degree), electronic ground states, and the relative energies (in kilocalories per mole) of the possible product and isomer calculated at the BPW91/6-311+G(d)-SDD level.

stepwise annealing behavior of the product absorptions are also shown in the figures and will be discussed below.

Quantum chemical calculations have been carried out for the possible isomers and electronic states of the potential product molecules. Figure 3 shows the optimized structures and electronic ground states. Table 2 reports a comparison of the observed and calculated IR frequencies and isotopic frequency ratios of the reaction product. Calculated vibrational frequencies and intensities of the potential products are listed in Table 3.

Laser ablation of a DyH_x target gives rise to a strong absorption at 1193.7 cm^{-1} and a weak absorption at 1247.1 cm^{-1} , which are due to DyH_2 .⁷ In addition to the absorptions due to dysprosium carbonyls observed in the experiments of laser ablation of Dy with CO and the dysprosium hydrides observed in the experiments of laser ablation of DyH_x , new absorptions at 1864.0 and 1086.0 cm^{-1} are observed in the experiments of laser ablation of DyH_x with CO. The absorptions at 1864.0 and

Table 2. Comparison of Observed and Calculated IR Frequencies (cm^{-1}) and Isotopic Frequency Ratios of the Reaction Product

Species	Mode ^{a)}	Experimental			Calculated			
		Freq/cm ⁻¹	<i>R</i> (12/13)	<i>R</i> (16/18)	Method	Freq/cm ⁻¹	<i>R</i> (12/13)	<i>R</i> (16/18)
HDyCO	CO str.	1864.0 (<i>A</i> = 0.015)	1.0220	1.0247	BPW91	1864.5	1.0229	1.0244
					BP86	1861.4	1.0229	1.0244
	DyH str.	1086.0 (<i>A</i> = 0.016)			BPW91	1278.5		
					BP86	1275.0		

a) str. = stretching mode.

Table 3. Ground Electronic States, Point Groups, Vibrational Frequencies (cm^{-1}) and Intensities (km mol^{-1}) of the Reaction Products and Isomers Calculated at the BPW91/6-311+G(d)-SDD Level (Only the Frequencies Above 400 cm^{-1} are Listed)

Species	Elec state	Point group	Frequency (intensity, mode)
HDyCO	$^4A''$	C_s	1864.5 (663, A'), 1278.5 (839, A')
HDyOC	$^6A'$	C_s	2124.3 (102, A'), 1239.4 (396, A')

1086.0 cm^{-1} appear on sample deposition, visibly increase on sample annealing at 25 K, and decrease on annealing at 30 and 35 K (Table 1 and Figure 1). The observed intensities (A : absorbance) of 1864.0 cm^{-1} band at 4, 25, 30, and 35 K are 0.004, 0.015, 0.01, and 0.007, respectively, and the observed intensities (A : absorbance) of 1086.0 cm^{-1} band at 4, 25, 30, and 35 K are 0.005, 0.016, 0.012, and 0.008, respectively. The absorptions at 1864.0 and 1086.0 cm^{-1} can be grouped together to one species, based on the growth/decay characteristics as a function of changes of experimental conditions. The 1864.0 cm^{-1} band shifts to 1823.9 cm^{-1} with $^{13}\text{C}^{16}\text{O}$ and to 1819.0 cm^{-1} with $^{12}\text{C}^{18}\text{O}$, exhibiting isotopic frequency ratios ($^{12}\text{C}^{16}\text{O}/^{13}\text{C}^{16}\text{O}$, 1.0220; $^{12}\text{C}^{16}\text{O}/^{12}\text{C}^{18}\text{O}$, 1.0247) characteristic of C–O stretching vibration. As shown in Figure 2, the mixed $^{12}\text{C}^{16}\text{O} + ^{13}\text{C}^{16}\text{O}$ and $^{12}\text{C}^{16}\text{O} + ^{12}\text{C}^{18}\text{O}$ isotopic spectra only provide the sum of pure isotopic bands, which indicates that only one CO subunit is involved in this mode. The position of the 1086.0 cm^{-1} band indicates a Dy–H stretching vibration. Doping with CCl_4 has no effect on these bands, which suggests that the product is neutral.⁴ The 1864.0 and 1086.0 cm^{-1} bands are therefore assigned to the C–O and Dy–H stretching vibrations of the neutral HDyCO molecule, respectively.

Our calculations predict that the HDyCO has an $^4A''$ ground state with C_s symmetry, which is 38.9 kJ mol^{-1} lower in energy than the HDyOC isomer (Figure 3). The doublet and sextet states are predicted to have imaginary frequencies and are much higher in energy than the quartet state at the present level of calculations. The Dy–O bond length of HDyOC is predicted to be 5.480 Å , indicating that the molecule is not formed. The Dy–H and C–O bond lengths of ground-state HDyCO are 2.068 and 1.176 Å , respectively, which are 0.048 and 0.048 Å longer than those of DyH and CO calculated at the same level. The quartet HDyCO molecule has a $(\text{core})-(1a')^2(2a')^2(3a')^2(4a')^2(5a')^2(6a')^2(7a')^2(8a')^2(9a')^2(10a'')^2-(11a')^2(12a')^2(13a')^2(14a')^2(15a')^1(15a'')^1(16a'')^1(16a')^1(17a')^2-(18a')^1(18a'')^1(19a'')^1(19a')^1(20a')^2(21a')^2(22a'')^1(22a')^1(23a')^1-$

$(23a'')^1(24a'')^1(24a')^1(25a')^1(25a'')^1(26a')^1(27a'')^1(28a')^1$ electronic configuration. The spin contamination ($\langle S^2 \rangle$) is predicted to be 5.3988. As shown in Figure 4, the alpha-spin highest occupied molecular orbital (HOMO) is largely H 1s and Dy 6s in character and is nonbonding. The beta HOMO in the HDyCO molecule is a Dy–C π -bonding orbital, which is responsible for the stability of the molecule. The NBO analysis results show that the Dy atom within the HDyCO molecule has a $(\text{core})6s^{1.05}4f^{9.11}5d^{0.36}6p^{0.02}7s^{0.04}5f^{0.01}$ natural electron configuration. C–O and the Dy–H stretching vibrational frequencies are calculated to be 1864.5 and 1278.5 cm^{-1} (Tables 2 and 3), which must be scaled down by 0.999 and 0.849 to fit the experimental observations, respectively. The calculated frequencies are harmonic while the experimental frequencies are fundamental that are affected by the anharmonicity of the potential energy surface, which will result in some difference between the calculated values and experimental observations. The calculated $^{12}\text{C}^{16}\text{O}/^{13}\text{C}^{16}\text{O}$ and $^{12}\text{C}^{16}\text{O}/^{12}\text{C}^{18}\text{O}$ isotopic frequency ratios are also consistent with the experimental observations. These agreements between the experimental and calculated vibrational frequencies, and isotopic shifts confirm the identification of the HDyCO molecule from the matrix IR spectra.

Laser ablation of a DyH_x target may produce dysprosium hydrides such as DyH and DyH₂ as well as Dy and H atoms. It is also possible that the DyCO molecule is formed by the reaction of Dy with CO. Therefore, the following two plausible reaction mechanisms can be proposed. One mechanism is that DyH is co-deposited with CO to form the HDyCO complex during sample deposition (Figure 1). Another mechanism is that DyCO reacts with atomic H to form the HDyCO complex. The HDyCO species markedly increases on annealing, suggesting that the reactions to form the HDyCO complex are spontaneous.

Conclusion

Reactions of laser-ablated dysprosium hydride with CO in excess argon have been studied using matrix-isolation infrared spectroscopy. On the basis of the isotopic shifts and splitting patterns, the HDyCO molecule has been characterized. Density functional theory calculations have been performed, which lend support to the experimental assignment of the infrared spectra. In addition, a plausible reaction mechanism for the formation of the product has been proposed.

The authors thank the reviewers for their valuable suggestions and comments. This work was supported by a Grant-in-Aid for Scientific Research (B) (Grant No. 17350012) from the Ministry of Education, Culture, Sports, Science and Tech-

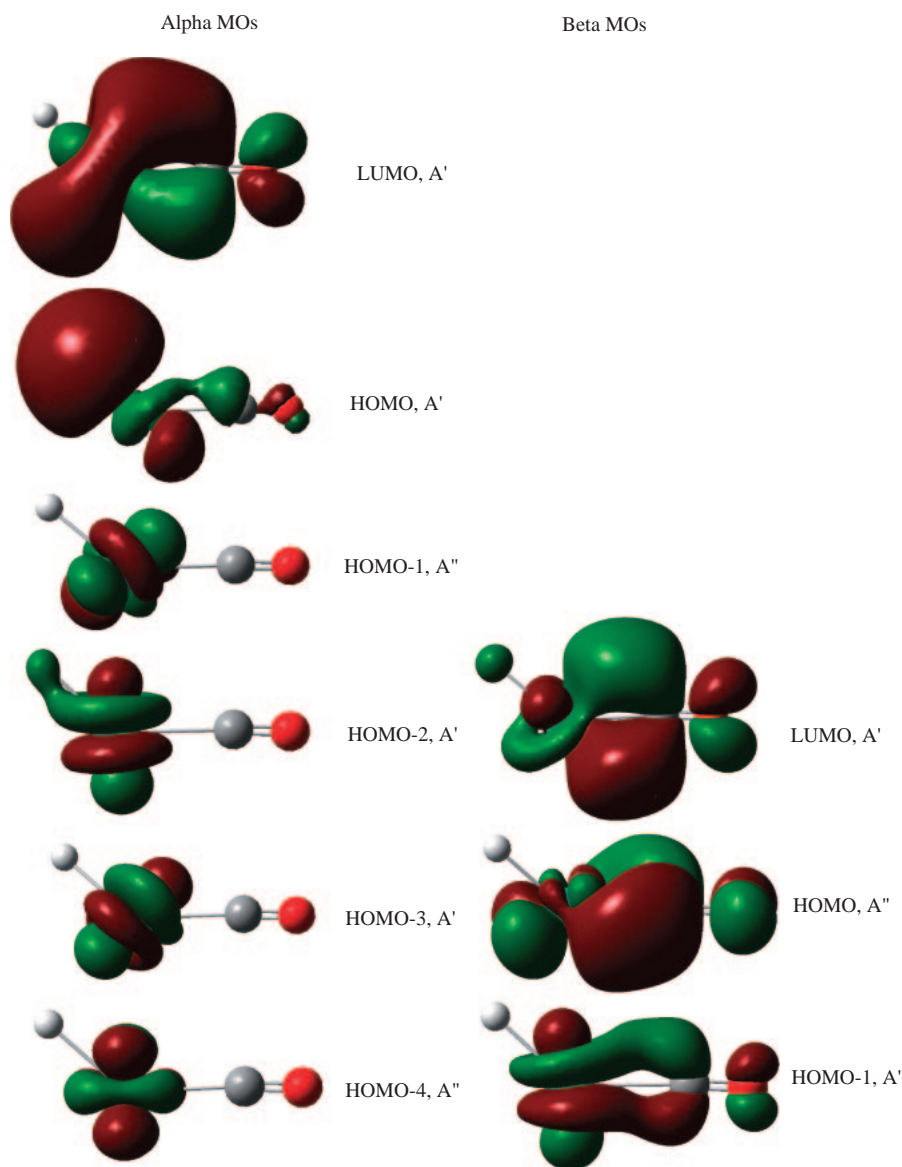


Figure 4. Molecular orbital pictures of quartet HDyCO calculated at the BPW91/6-311+G(d)-SDD level.

nology (MEXT) of Japan and Marubun Research Promotion Foundation. Y.-L.T. thanks JASSO and Kobe University for an Honors Scholarship.

References

- 1 F. A. Cotton, G. Wilkinson, C. A. Murillo, M. Bochmann, *Advanced Inorganic Chemistry*, 6th ed., Wiley, New York, **1999**.
- 2 a) E. L. Muetterties, J. Stein, *Chem. Rev.* **1979**, 79, 479. b) W. Tumas, B. Gitlin, A. M. Rosan, J. T. Yardley, *J. Am. Chem. Soc.* **1982**, 104, 55.
- 3 G. B. Richter-Addo, P. Legzdins, J. Burstyn, *Chem. Rev.* **2002**, 102, 857.
- 4 M. Zhou, L. Andrews, C. W. Bauschlicher, Jr., *Chem. Rev.* **2001**, 101, 1931.
- 5 L. Jiang, X. Jin, M. F. Zhou, Q. Xu, *J. Phys. Chem. A*, in press.
- 6 a) L. Schlapbach, A. Züttel, *Nature* **2001**, 414, 353. b) A. Percheron-Guégan, C. Lartigue, J. C. Achard, *J. Less-Common Met.* **1985**, 109, 287. c) J. H. N. Van Vucht, F. A. Kuijpers, H. C. A. M. Bruning, *Philips Res. Rep.* **1970**, 25, 133.
- 7 a) S. P. Willson, L. Andrews, *J. Phys. Chem. A* **2000**, 104, 1640. b) L. Andrews, *Chem. Soc. Rev.* **2004**, 33, 123.
- 8 a) *New Syntheses with Carbon Monoxide*, ed. by J. Falbe, Springer-Verlag, Berlin, **1980**. b) K. A. Mahmoud, A. J. Rest, H. G. Alt, *J. Chem. Soc., Dalton Trans.* **1984**, 187. c) V. Jonas, W. Thiel, *J. Chem. Phys.* **1996**, 105, 3636. d) G. Bor, *Inorg. Chim. Acta* **1967**, 1, 81. e) R. L. Sweany, *J. Am. Chem. Soc.* **1982**, 104, 3739.
- 9 a) H.-F. Oetjen, V. M. Schmidt, U. Stimming, F. Trila, *J. Electrochem. Soc.* **1996**, 143, 3838. b) L. Niedrach, D. Mckee, J. Paynter, I. Danzig, *Electrochem. Technol.* **1967**, 5, 318. c) M. Watanabe, S. Motoo, *J. Electroanal. Chem.* **1975**, 60, 275. d) H. A. Gasteiger, N. Markovic, P. N. Ross, E. J. Cairns, *J. Phys. Chem.* **1994**, 98, 617.
- 10 X. Wang, L. Andrews, *J. Phys. Chem. A* **2000**, 104, 9892.
- 11 Y.-L. Teng, Q. Xu, *J. Phys. Chem. A* **2007**, 111, 13380.
- 12 a) T. R. Burkholder, L. Andrews, *J. Chem. Phys.* **1991**, 95,

8697. b) M. Zhou, N. Tsumori, L. Andrews, Q. Xu, *J. Phys. Chem. A* **2003**, 107, 2458. c) L. Jiang, Q. Xu, *J. Chem. Phys.* **2005**, 122, 034505.

13 M. J. Frisch, G. W. Trucks, H. B. Schlegel, G. E. Scuseria, M. A. Robb, J. R. Cheeseman, J. A. Montgomery, Jr., T. Vreven, K. N. Kudin, J. C. Burant, J. M. Millam, S. S. Iyengar, J. Tomasi, V. Barone, B. Mennucci, M. Cossi, G. Scalmani, N. Rega, G. A. Petersson, H. Nakatsuji, M. Hada, M. Ehara, K. Toyota, R. Fukuda, J. Hasegawa, M. Ishida, T. Nakajima, Y. Honda, O. Kitao, H. Nakai, M. Klene, X. Li, J. E. Knox, H. P. Hratchian, J. B. Cross, C. Adamo, J. Jaramillo, R. Gomperts, R. E. Stratmann, O. Yazyev, A. J. Austin, R. Cammi, C. Pomelli, J. W. Ochterski, P. Y. Ayala, K. Morokuma, G. A. Voth, P. Salvador, J. J. Dannenberg, V. G. Zakrzewski, S. Dapprich, A. D. Daniels, M. C. Strain, O. Farkas, D. K. Malick, A. D. Rabuck, K. Raghavachari, J. B. Foresman, J. V. Ortiz, Q. Cui, A. G. Baboul,

S. Clifford, J. Cioslowski, B. B. Stefanov, G. Liu, A. Liashenko, P. Piskorz, I. Komaromi, R. L. Martin, D. J. Fox, T. Keith, M. A. Al-Laham, C. Y. Peng, A. Nanayakkara, M. Challacombe, P. M. W. Gill, B. Johnson, W. Chen, M. W. Wong, C. Gonzalez, J. A. Pople, *Gaussian 03, Revision B.04*, Gaussian, Inc., Pittsburgh, PA, **2003**.

14 a) J. P. Perdew, *Phys. Rev. B* **1986**, 33, 8822. b) A. D. Becke, *Phys. Rev. A* **1988**, 38, 3098. c) J. P. Perdew, K. Burke, Y. Wang, *Phys. Rev. B* **1996**, 54, 16533.

15 a) R. Krishnan, J. S. Binkley, R. Seeger, J. A. Pople, *J. Chem. Phys.* **1980**, 72, 650. b) M. J. Frisch, J. A. Pople, J. S. Binkley, *J. Chem. Phys.* **1984**, 80, 3265.

16 a) M. Dolg, U. Wedig, H. Stoll, H. Preuss, *J. Chem. Phys.* **1987**, 86, 866. b) M. Dolg, H. Stoll, H. Preuss, *J. Chem. Phys.* **1989**, 90, 1730.